

## Step changes in the flood frequency curve: Process controls

M. Rogger,<sup>1</sup> H. Pirkel,<sup>2</sup> A. Viglione,<sup>1</sup> J. Komma,<sup>1</sup> B. Kohl,<sup>3</sup> R. Kirnbauer,<sup>1</sup> R. Merz,<sup>4</sup> and G. Blöschl<sup>1</sup>

Received 22 July 2011; revised 23 March 2012; accepted 8 April 2012; published 24 May 2012.

[1] Empirical distribution functions of flood peaks in small catchments sometimes show discontinuities in the slope; that is, the largest flood peaks are significantly larger than the rest of the record. The aim of this paper is to understand whether these discontinuities, or step changes, can be a consistent effect of hydrological processes. We conducted field surveys in two Austrian alpine catchments 73 km<sup>2</sup> in size to map the spatial patterns of surface runoff generation and hydrogeologic storage. On the basis of this information, we selected the parameters of a distributed continuous runoff model, which is designed to simulate well the point when the storage capacity of the catchment is exhausted. Then we calibrated a stochastic rainfall model and performed Monte Carlo simulations of runoff to generate flood frequency curves for the two catchments. The curves exhibit a step change around a return period of 30 years. An analysis of the storage capacities suggests that this step change is due to a threshold of storage capacity being exceeded, which causes fast surface runoff in large parts of the catchments. The threshold occurs when the storage within the catchment is spatially rather uniform. To identify step changes, reliable estimates of the catchment storage capacity are needed on the basis of detailed hydrogeological information. The occurrence of a step change is of importance for estimating low-probability floods since the flood estimates with the step change accounted for can be significantly different from those based on commonly used distribution functions. We therefore suggest that step changes in the flood frequency curve of small catchments can be real and their possible presence should be taken into account in design flood estimation.

**Citation:** Rogger, M., H. Pirkel, A. Viglione, J. Komma, B. Kohl, R. Kirnbauer, R. Merz, and G. Blöschl (2012), Step changes in the flood frequency curve: Process controls, *Water Resour. Res.*, 48, W05544, doi:10.1029/2011WR011187.

### 1. Introduction

[2] Estimating low-probability floods is fundamental for many practical engineering applications. The flood estimates are either based on fitting a statistical distribution to observed flood peaks or on rainfall-runoff modeling. If a long stationary flood record is available the statistical approach is usually preferred and has therefore been established as the “standard approach” to flood frequency analysis [Klemeš, 1993]. In many cases though flood records are short and one has to extrapolate far beyond the flood data record to the tail of the distribution as low-probability floods are of most interest. In this context a number of authors have argued that, particularly for short records, it is important to account for the hydrological processes occurring in the catchment of interest rather than resort to pure statistical extrapolation [Katz *et al.*, 2002; Klemeš, 1993].

A process-based approach to flood frequency estimation has recently been advocated by Merz and Blöschl [2008a, 2008b] and A. Viglione *et al.* (Flood frequency hydrology: 3. Bayesian analysis, submitted to *Water Resources Research*, 2012) with the “flood frequency hydrology” approach that introduces a temporal, spatial and causal information expansion beyond traditional flood frequency statistics.

[3] If a statistical distribution is fit to a flood data sample it is usually assumed that the distribution is smooth. However, the empirical distribution functions of measured runoff data sometimes show discontinuities in the slope. As an example, Figure 1 shows runoff data from two small catchments in the Austrian Alps. In both cases a few events have been observed that are significantly larger than the rest of the floods causing a sharp bend in the empirical distribution function. If this sharp bend is only shown by a few data points as in the Gurglbach catchment (Figure 1a), it could be argued that this is due to sampling uncertainty and the empirical return periods of these events should be larger than what the plotting position formula (in this case Weibull) gives. In the case of the Loisach catchment though (Figure 1b) the step change is indicated by a larger number of data points so it is more likely that it is the result of hydrological processes occurring in the catchment. This gives rise to an interesting question whether observed step changes are real or simply a sampling artifact. From a theoretical perspective this is extremely important since step

<sup>1</sup>Institute for Hydraulic Engineering and Water Resources Management, Vienna University of Technology, Vienna, Austria.

<sup>2</sup>Technical Office for Geology Dr. Herbert Pirkel, Vienna, Austria.

<sup>3</sup>Department of Natural Hazards and Alpine Timberline, Federal Research and Training Centre for Forests, Natural Hazards and Landscape, Innsbruck, Austria.

<sup>4</sup>Department for Catchment Hydrology, Helmholtz Centre for Environmental Research, Halle, Germany.

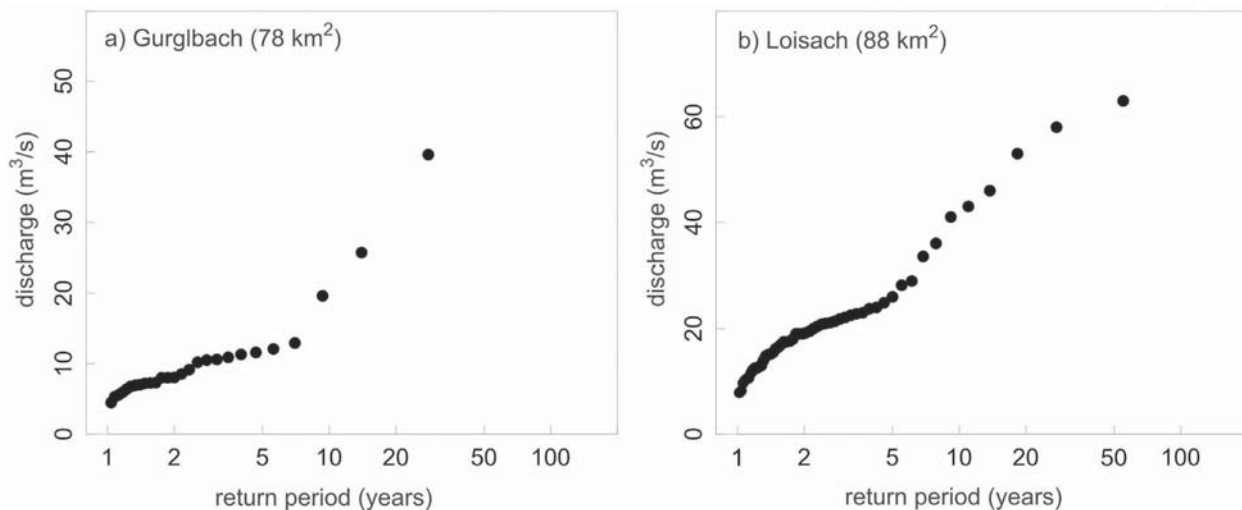


**Figure 1.** Empirical flood frequency curves of (a) the Gurglbach and (b) Loischach catchments. Maximum annual floods: 27 years of records in the Gurglbach catchment and 54 years of records in the Loischach catchment. Note the step changes at a return period of about 8 years.

changes, if only indicated by a few data points (Gurglbach example; Figure 1a), are not taken into account in traditional flood frequency statistics. Although more complex statistical distributions exist that allow for such step changes, their parameters are difficult to estimate, in particular if only a few floods larger than the breakpoint in the flood frequency curve have been observed. From a practical perspective this is similarly important as accounting for step changes would give in most cases larger flood estimates than fitting a smooth distribution function.

[4] If step changes in the flood frequency curves are real, they might be related to threshold processes that refer to a rapid changeover from one state to another. It has often been proposed that during extreme flood events processes are significantly different from small or medium events [Rossi *et al.*, 1984; Klemeš, 1993; Gutknecht, 1994]. Threshold processes occur in hydrological and geoecosystems and are linked to hazards such as flooding or erosion [Zehe and Sivapalan, 2009]. One of the first to describe runoff generation that is influenced by threshold behavior was Horton [1933], who showed that in case rainfall intensity exceeds the infiltration capacity of a soil, a sudden increase in surface runoff can be observed (Hortonian overland flow). Another well-known runoff generation mechanism that can have a similar effect is the saturation excess mechanism [Dunne and Black, 1970] that develops when soils become saturated and any additional precipitation transforms into runoff. In the last decades threshold processes have been observed in many experimental catchments causing for instance a sudden increase of subsurface stormflow at a certain threshold of rainfall depth [Whipkey, 1965; Tromp-van Meerveld and McDonnell, 2006] or at a certain soil moisture index [Detty and McGuire, 2010]. A possible explanation for the process causing this phenomenon is given by the fill and spill hypothesis [Tromp-van Meerveld and McDonnell, 2006] that implies that bedrock depressions at hillslopes have to be filled during a rainfall event before subsurface areas can become connected and produce a

sudden increase in subsurface stormflow. These studies refer to the local scale, but threshold processes have also been discussed on a catchment scale mainly referring to runoff generation depending on soil moisture conditions, macropore flow and spatially variable precipitation in relation to Horton overland flow [Zehe and Blöschl, 2004; Zehe *et al.*, 2005] or examining water residence time in catchments [McGuire *et al.*, 2005].

[5] However, only very few studies have examined the effects of changes in the process type on the shape of the flood frequency distribution. For instance, Sivapalan *et al.* [1990] suggested that for catchments where saturation excess (Dunne) runoff generation dominates at low-return periods and infiltration excess (Horton) runoff generation at high-return periods a transition from the saturation excess curve to the infiltration excess curve occurs at a certain return period resulting in a step change in the flood frequency distribution. Also, Blöschl and Sivapalan [1997] showed that assuming a simplified threshold process, where the runoff coefficient leaps from a lower to a higher value at a certain rainfall threshold, can result in a “kink” or step change in the flood frequency distribution. While these papers have provided interesting initial steps toward analyzing step changes in the tail of the flood frequency curve they have invariably been performed on hypothetical catchments. It would be interesting to see whether these step changes can actually occur in real catchments and what the controls of these step changes are.

[6] The main aim of this paper is to understand whether step changes in the flood frequency curve can be real and are related to hydrological processes in the catchment or are an artifact of sampling uncertainty. To this end a detailed runoff process study for two small adjacent alpine catchments is presented, where it is unclear from the flood data alone whether such a step change occurs. The flood frequency distribution of the two catchments is obtained by a derived flood frequency approach [Eagleson, 1972; Sivapalan *et al.*, 2005; Allamano *et al.*, 2009]. The main strength of the

derived flood frequency approach is to help understand the process controls of flood frequency behavior, especially the ability to focus on a threshold change of dominant processes with increasing return period [Sivapalan *et al.*, 1990; Blöschl and Sivapalan, 1997; Viglione *et al.*, 2009]. In both catchments detailed field observations on hydrogeologic storage and surface runoff of the catchments were available and used for model parameter selection.

## 2. Model and Data

### 2.1. Study Area

[7] The study was performed in two small alpine catchments, the Weerbach and Wattenbach catchments, which are both about 73km<sup>2</sup> in size. Both catchments are tributaries to the Inn River and are located in Tyrol in the Austrian Alps. The elevations in the catchments range from 500 to 2900 m above sea level, the mean annual precipitation is about 1500 mm. The largest floods in the region occur in the months from June to September and are mainly synoptic flood events caused by frontal events with long duration and large spatial extent [Merz and Blöschl, 2003].

### 2.2. Rainfall Runoff Model

[8] The rainfall-runoff model used in this paper is a spatially distributed continuous water balance model on a pixel basis [Blöschl *et al.*, 2008] similar to the models of Bergström and Forsman [1973] and Nielsen and Hansen [1973]. The model consists of a snow routine, a soil moisture routine and a flow routing routine. The snow routine represents snow accumulation and snow melt by a simple degree-day concept that divides precipitation into snow  $P_s$  and rainfall  $P_r$  and accounts for snowmelt  $M$ . Rainfall and snowmelt are split into a component  $dS$  that increases soil moisture of a top layer  $S_s$  and a component that contributes to runoff  $Q_p$ . The partition into the two components is

computed by a nonlinear function depending on the maximum soil moisture storage  $L_s$ . The parameter  $\beta$  describes the linearity of runoff generation.

$$dQ = \left( \frac{S_s}{L_s} \right)^\beta (P_r + M)$$

[9] Soil moisture can only decrease by evapotranspiration which is estimated on the basis of the potential evapotranspiration. Runoff routing on the hillslope is represented by an upper zone and two lower reservoirs (Figure 2). The component of rainfall and snowmelt  $Q_p$  that contributes to runoff enters the upper zone reservoir and leaves this reservoir through three paths: percolation to the lower reservoirs defined by the percolation rate  $c_p$ , outflow from the reservoir with a fast storage coefficient  $k_1$  and additionally, when the threshold  $L_1$  is exceeded, outflow through a further outlet with a very fast storage coefficient  $k_0$ . The percolation into the two lower storages is split into two components by the fraction  $\alpha_p$ . The outflow from the lower storages is given by the storage coefficients  $k_2$  and  $k_3$ , respectively. Total runoff  $Q_t$  of one pixel is the sum of the outflows from the different reservoirs.  $Q_0$  represents surface runoff and near surface runoff,  $Q_1$  interflow,  $Q_2$  a lower soil zone or shallow groundwater flow and  $Q_3$  a deeper groundwater flow.

$$Q_t = Q_0 + Q_1 + Q_2 + Q_3$$

[10] Runoff routing in the stream network is expressed by cascades of linear reservoirs. To this purpose the catchment is subdivided into different subcatchments that are connected by a simplified river network. In order to be able to represent the fast runoff processes in the small alpine catchments of the Weerbach and Wattenbach well, a high

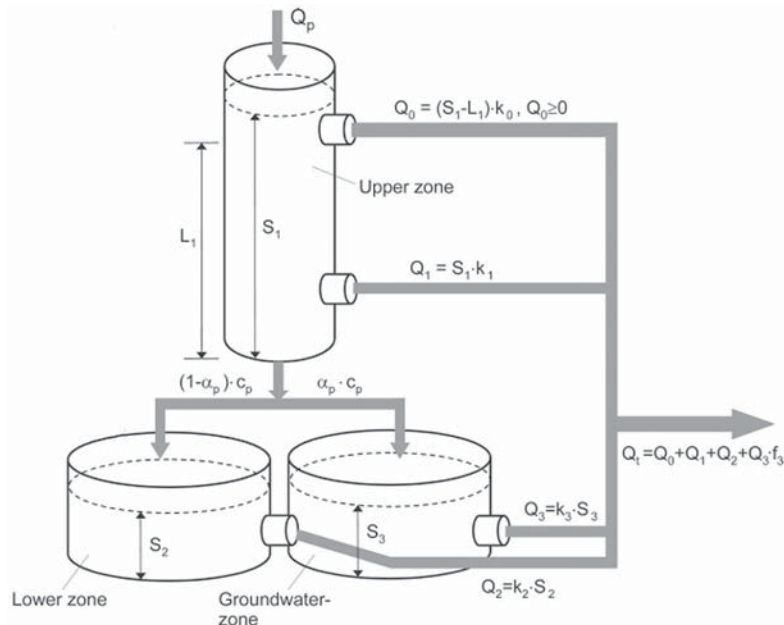


**Figure 2.** Structure of the rainfall-runoff model on the pixel scale.  $S$  are the storage states, and  $Q$  are fluxes [Blöschl *et al.*, 2008].

temporal resolution of 15 min and spatial resolution of 200 m  $\times$  200 m pixels were chosen in the model.

### 2.3. Input Data

[11] Rainfall data, temperature data and estimated potential evapotranspiration for the period 1985 to 2007 were used as inputs to the model. The Wattener Lizum rainfall station with data at a resolution of 5 min is located in the upper Wattenbach catchment. The data series was used for both the Wattenbach and the neighboring Weerbach catchments. The measured point rainfall was taken as areal rainfall input to the model, because the main interest was in simulating extremes, so smoothing effects of interpolation should be avoided. Moreover, the catchments are rather small and most floods in the region are synoptic floods caused by frontal events [Merz and Blöschl, 2003] so that the assumption on spatially uniform rainfall is reasonable. Air temperatures were interpolated from 20 surrounding stations at a resolution of 15 min accounting for elevation by a regional regression. Potential evapotranspiration was estimated by the modified Blaney Criddle method [Deutscher Verband für Wasserwirtschaft und Kulturbau, 1996] as a function of air temperature. In both catchments runoff measurements at a resolution of 15 min were available from 1979 to 2007.

### 2.4. Strategy of Parameter Identification

[12] The parameters of the model were selected on the basis of the approach proposed by Reszler *et al.* [2006]. The main goal was to capture runoff processes in as much detail as possible. The approach consists of four steps: (1) a priori choice of upper zone reservoir and soil storage parameters based on field information (step 1a), a priori choice of lower zone reservoir and groundwater storage parameters based on field information (step 1b), and consistency check of the parameters with respect to surface

runoff response units and hydrogeologic response units (step 1c), (2) manual calibration of the parameters by comparing simulated and observed runoff on a seasonal scale, (3) manual calibration of the parameters by comparing simulated and observed runoff on the event scale for different types and magnitudes of events, and (4) consistency check of calibrated parameters with field information and possibly another iteration to step 1.

[13] The proposed strategy of parameter selection is mainly based on field data in order to accommodate a qualitative understanding of runoff generation processes in the catchments. The strategy also involves some element of calibration which in this case does not refer to the optimizing of an objective function. Instead, the a priori model parameters based on field information were only slightly changed to preserve the conceptualization of dominant processes in the model. Optimizing the parameters based on runoff only would provide better hydrographs fits but a poorer representation of the runoff mechanisms as observed in the field.

#### 2.4.1. Step 1a: A Priori Choice of Upper Zone Reservoir and Soil Storage Parameters

[14] For the a priori choice of the parameters of the upper zone reservoir and soil storage the catchments were subdivided into surface runoff response units (SRRU) on the basis of the method of Markart *et al.* [2004]. In this rule-based method, surface runoff is estimated from vegetation, soil characteristics, land use, and indicator plants. The parameters of the rules were obtained by Markart *et al.* [2004] in a number of field irrigation experiments. Figure 3 shows three typical cases of different runoff generation classes for high alpine catchments: Debris areas (Figure 3a) for instance yield almost no surface runoff (runoff coefficients between 0 and 0.1). Green alder populations (Figure 3b), on the other hand, are indicator plants for high runoff coefficients of 0.5

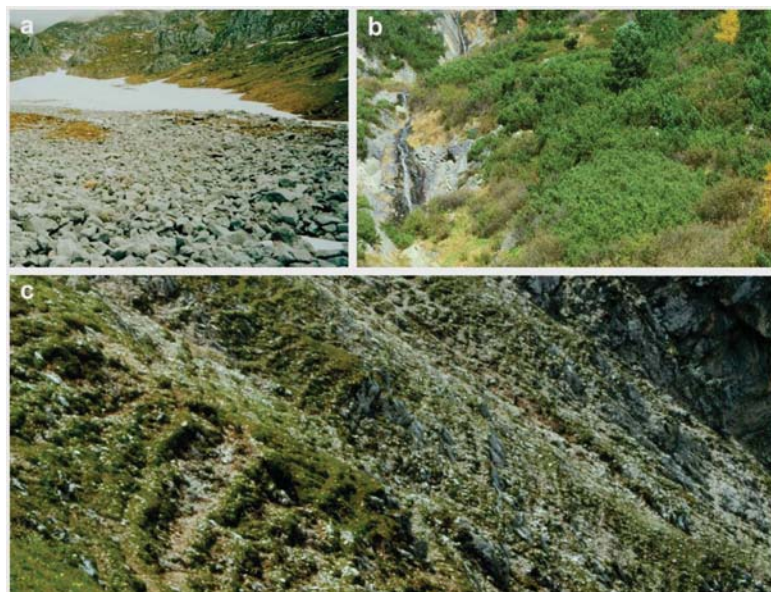


**Figure 3.** (a) Debris fan, (b) green alder, and (c) alpine grass influenced by grazing as indicators for surface runoff coefficients [Markart *et al.*, 2004].

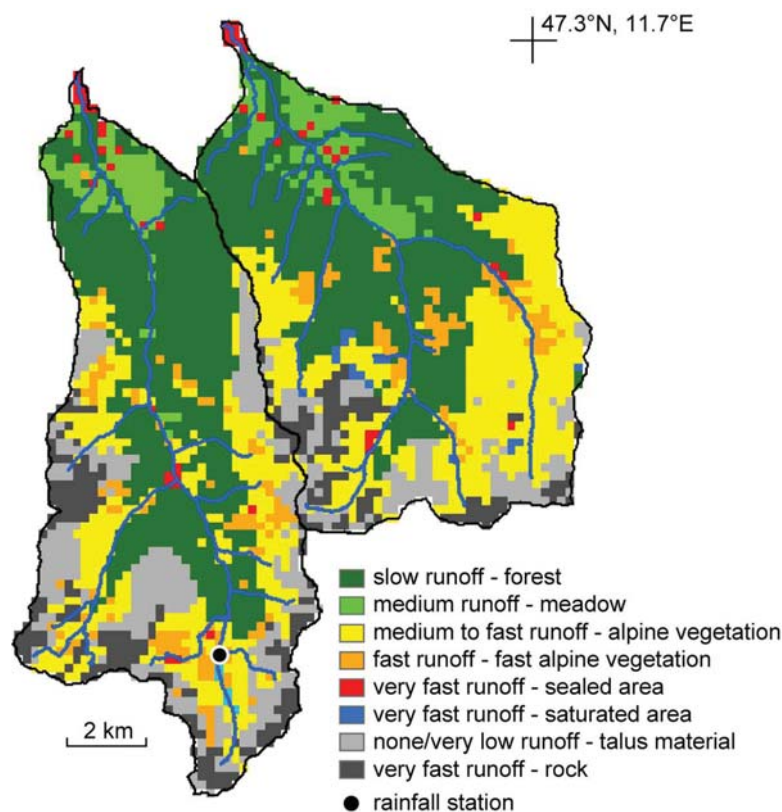
to 0.75 since they occur on shallow soils over bedrock. Also typical are alpine grass areas (Figure 3c) influenced by cattle grazing. Because of the grazing activities the soil is compacted resulting in high runoff coefficients of 0.5 to 0.8. Other examples (not shown) are forested areas which are generally associated with low runoff coefficients (0.1 to 0.5) since they occur on deeper soils or sealed areas and bare rock with nearly no storage capacity that have high runoff coefficients up to 1. Note that runoff coefficients were not used in the model but are an indication of event runoff production in the catchment that should be reflected in the upper zone reservoir and soil storage parameters.

[15] On the basis of this information eight surface runoff response classes were defined ranging from low runoff in forests to very fast runoff from rocks (Figure 4). Each pixel of the model was assigned to one of the classes and each class has one set of parameters in the model. This subdivision was used for the definition of the parameters  $L_s$ ,  $\beta$ ,  $L_1$ ,  $k_0$ ,  $k_1$ , which determine surface runoff and interflow. For instance, for the low runoff, forest response unit, where a slow runoff generation is expected, maximum soil moisture storage  $L_s$  was set between 100 and 150 mm, and a  $\beta$  value of 4 representing strongly nonlinear runoff generation. For the same unit, relatively high storage coefficients were chosen, i.e.,  $k_0$  between 10 and 20 h and  $k_1$  between 100 and 200 h. The upper storage threshold  $L_1$  was set between 100 and 140 mm. All these parameters represent a rather slow runoff response of each pixel in the model. A very fast

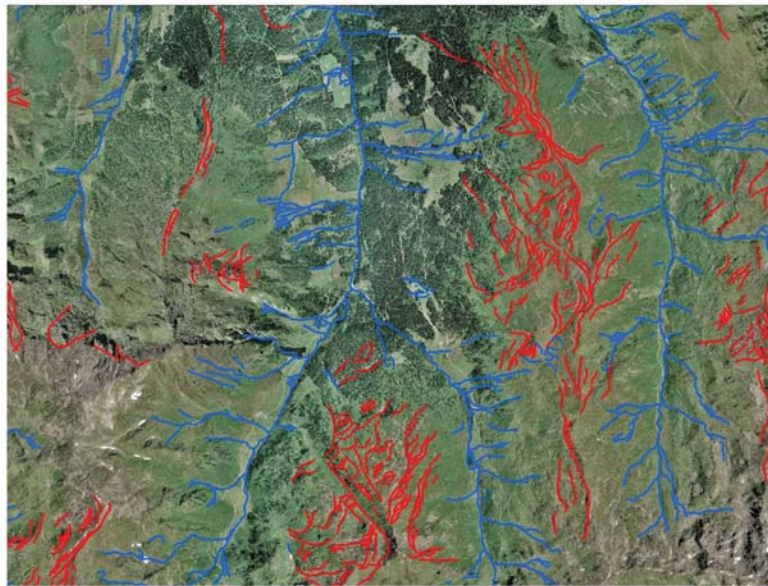
response unit such as very fast runoff, rock, on the other hand has a low storage capacity and fast runoff response. In this case the maximum soil moisture storage  $L_s$  was set between 5 and 30 mm and  $\beta$  was chosen as 1 to enable fast runoff generation. The threshold  $L_1$  of the upper reservoir was set between 1 and 10mm and the storage coefficients  $k_0$  between 1 and 5 h and  $k_1$  between 20 and 40 h. These values were chosen to represent the fast surface runoff response as expected from the field surveys. The remaining parameters were chosen in a similar way to account for the understanding of the runoff generation processes obtained during the field trips.

#### 2.4.2. Step 1b: A Priori Choice of Lower Zone Reservoir and Groundwater Storage Parameters

[16] The parameters for the lower zone and deep groundwater storage were estimated on the basis of hydrogeologic runoff process maps. These maps were obtained by a detailed assessment of orthophotos, geologic maps, hydrogeologic maps, digital terrain models and maps of unconsolidated sediments and refined in extensive field trips. First, the river network was determined from the orthophotos including nonpermanent micro channels (see blue lines Figure 5). A high surface runoff points toward areas with low storage capacities. In a second step the digital terrain model and the available geologic maps were used to delineate areas with deep mass movements and dispersed sediments, where one can assume that storage capacities are high (see red lines



**Figure 4.** Surface runoff response units (SRRU) in (left) the Wattenbach and (right) Weerbach catchments.



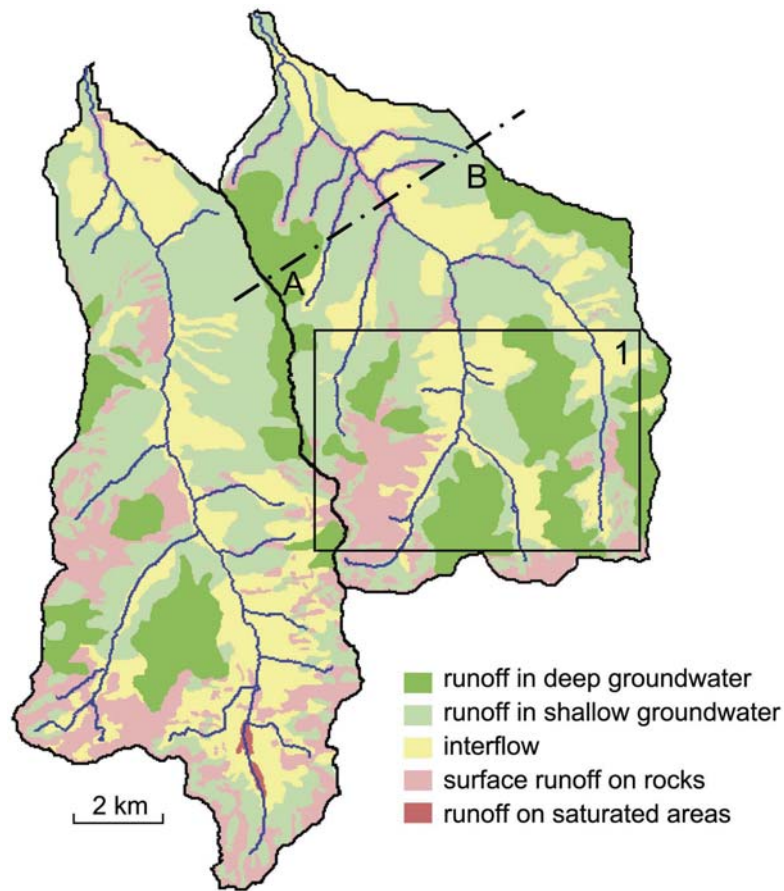
**Figure 5.** Weerbach catchment. Blue lines indicate the river network, and red lines indicate deep mass movements. The area is outlined in Figure 6 as a rectangle.

Figure 5). By combining the outcome of this analysis with the remaining geologic information different hydrogeologic response units (HGRU) were defined such as predominant runoff in deep groundwater, predominant runoff in shallow groundwater, predominant interflow, surface runoff on rocks and predominant runoff on saturated areas. Figure 6 shows the runoff process maps with the different hydrogeologic response units for the Weerbach and Wattenbach catchment which illustrate the areas that contribute to surface runoff during flood events and highlight areas with high storage potential. The maps were refined in field trips performing additional runoff measurements at selected points in the river network. The outcome of the geologic assessment gives an idea about the potential storage capacities of the catchment from a hydrogeologic point of view. The actual storage capacity also depends on the characteristics of the upper soil and land use, which were already considered in the parameter choice of the surface runoff response units. Figure 7 shows a cross section of how the runoff process maps help gain information on the parameter choice of the model indicating at which depth runoff processes take place. The cross section also illustrates qualitatively the different magnitudes of storage capacities of each area. The model parameters were chosen in a way that mimics these patterns. Specifically, the hydrogeologic information was used to choose the parameters  $c_p$ ,  $\alpha_p$ ,  $k_2$  and  $k_3$  which determine the shallow and deep groundwater flow. The main focus in the choice of parameters was on conserving the relation of the different magnitudes of storages of the areas to each other. Areas with deep groundwater flow have a high percolation rate  $c_p$  into the subsurface between 10 to 20 mm d<sup>-1</sup> and in the deeper groundwater storage with an  $\alpha_p$  value of 0.5 to 0.9, while the parameters for areas with predominant surface runoff on rocks were set in a way that mainly allows for flow on the surface with low percolation rates  $c_p$  of 1 to 3 mm d<sup>-1</sup> and low contribution to the deeper soil and groundwater flow given by an  $\alpha_p$  around 0. The storage parameters for the deep groundwater flow were

chosen between 800 to 3000 h and essentially only occur on areas with predominant groundwater flow. The shallow groundwater storage coefficients were set at 100 to 600 h with the low values for the shallow and faster reacting areas and the higher values for the deeper slower reacting areas. This is an example of how parameters for groundwater storages can be inferred from hydrogeologic field information which is important for representing catchment storage well.

#### 2.4.3. Step 1c: Consistency Check of the Parameters With Respect to Surface Runoff Response Units and Hydrogeologic Response Units

[17] The surface runoff response units and hydrogeologic response units were compared and, when needed, made consistent. For instance, pixels that belong to the surface runoff response unit very fast runoff, rock, also occur mainly on pixels from the hydrogeologic response unit predominant runoff on rocks so that only surface runoff is generated on these pixels. Areas from the surface runoff response unit no or very low runoff talus material, on the other hand, are expected not to contribute to surface runoff and mainly occur over pixels with predominant runoff in groundwater. In this case parameters were set in a way that mainly percolation to the deeper soil and groundwater storage occurs (high percolation rate  $c_p$ , high threshold  $L_1$ ). A third example are low runoff forest pixels which can occur over pixels from different hydrogeologic response units. If they occur over areas with predominant deep groundwater flow, they are expected to generate less interflow and surface runoff since percolation rates  $c_p$  are higher compared to the case when they occur on pixels with predominant interflow. By choosing the model parameters in this way the structure and depth at which flow processes take place in the catchment as shown by cross section in Figure 7 are adopted in the rainfall-runoff model considering also the upper soil storage characteristics as given by the surface runoff response units.



**Figure 6.** Hydrogeologic response units (HGRU) in (left) the Wattenbach and (right) Weerbach catchments. Rectangle highlights area of Figure 5.

**2.4.4. Step 2: Manual Calibration of the Parameters by Comparing Simulated and Observed Runoff on a Seasonal Scale**

[18] In order to reduce model bias, the model parameters were manually calibrated using observed runoff on a seasonal

scale during 2000–2007. Most parameters were changed only on the order of a few tens of percent. Figure 8 shows the runoff simulations for the Weerbach and Wattenbach catchments on a seasonal scale for the year 1990 which is part of the validation period 1985–1999. The results illustrate that

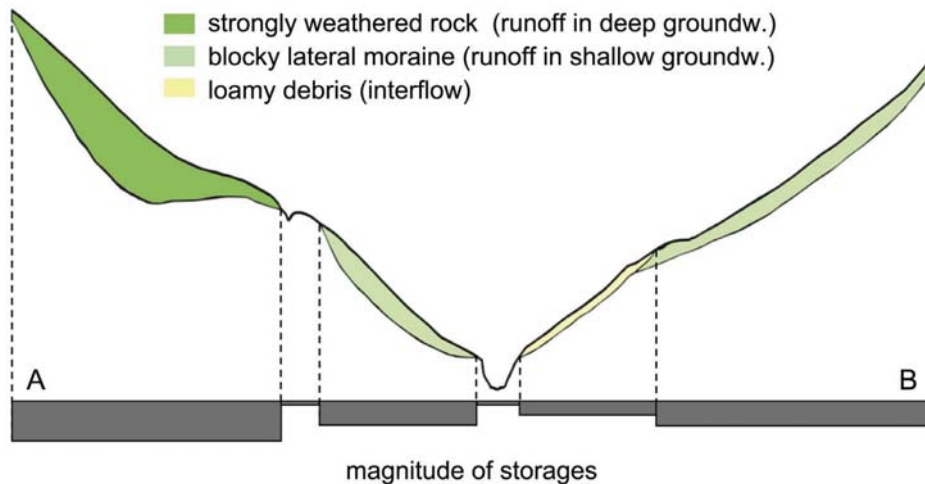


**Figure 7.** Weerbach catchment cross section (as highlighted in Figure 6) showing the magnitude of potential storage capacity.

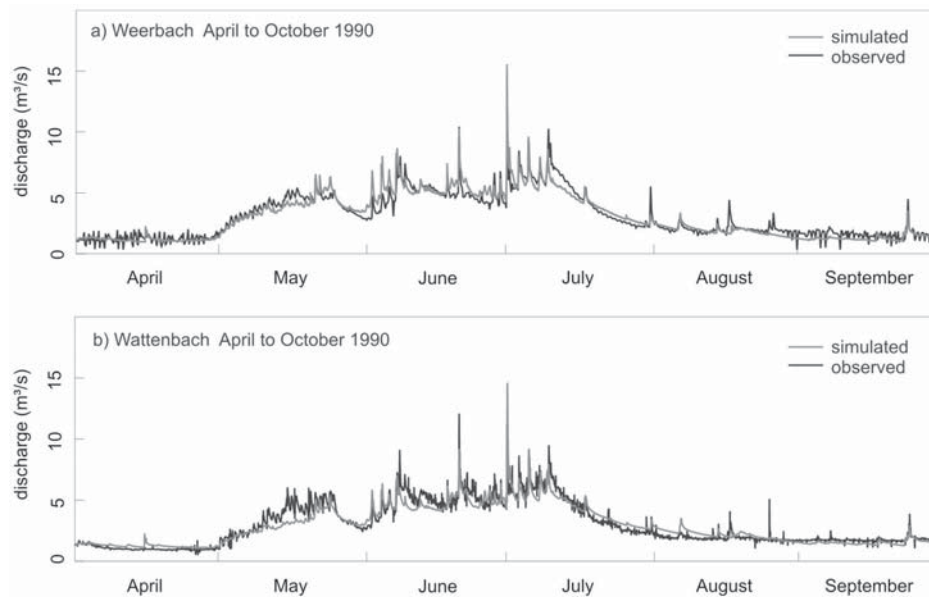


**Figure 8.** Runoff simulations for (a) the Weerbach and (b) Wattenbach catchments on a seasonal scale: April–October 1990 (validation period).

the model is able to capture the seasonal runoff dynamics and the water balance of the catchments well given the fact we are dealing with very small alpine catchments and low discharges. Low flows in both catchment are influenced by a small power plant and hence more variable than the simulations. Differences in the simulations and observations were analyzed and can be explained by the uncertainties in the measured rainfall and air temperature data.

#### 2.4.5. Step 3: Manual Calibration of the Parameters by Comparing Simulated and Observed Runoff on the Event Scale for Different Types and Magnitudes of Events

[19] As floods were of main interest in this study, some manual calibration of model parameters was also performed on the event scale. The same calibration and validation

periods were used as for the seasonal scale and the modifications of the parameters were of a similar order of magnitude. Figure 9 shows a comparison of the simulation and observations on the event scale for the flood event 2005. In both cases the receding limb of the floods is simulated well, which can be attributed to the fact that the storage capacities of the catchments are based on the detailed hydrogeologic information of the catchments. Note that break in the recession which is due to contributing areas with different responses time scales within the catchment. Similarly, the rising limbs are simulated well which suggests that the point when the storage capacity of the catchments is exceeded is captured. Floods in the two catchments are generated by different flood process types including frontal events, snow melt events, rain on snow events and convective events [Merz and Blöschl, 2003]. As all of them are of interest for

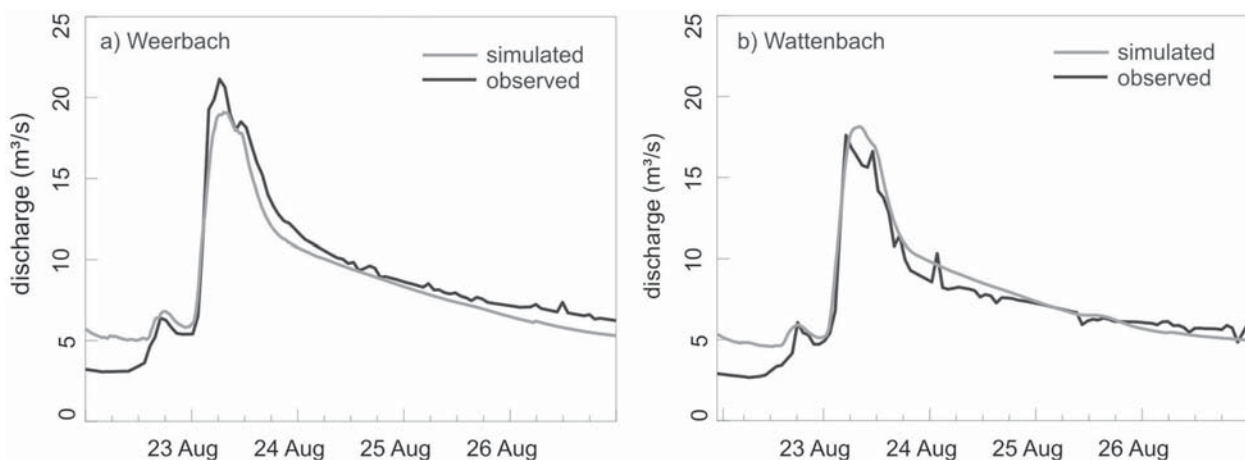


**Figure 9.** Runoff simulations for (a) the Weerbach and (b) Wattenbach catchments on an event scale (August 2005 event, calibration period).

flood frequencies the simulations of the individual types were compared independently with the observed floods. However, the largest floods occur in summer when no snow is involved. In a similar fashion, events of different magnitudes were compared to examine how the response characteristics change with the flood magnitudes.

[20] Figure 10 shows a comparison of the observed and simulated flood frequency statistics (calibration and validation periods) of the Weerbach and Wattenbach catchments. Overall there is a close correspondence between the simulations and the observations. It should be noted that the rainfall used for simulating the largest event (6 August 1985) in the two catchments was corrected. An analysis of the measured event rainfall at the Wattener Lizum station showed that the temporal pattern of the hyetograph did not fit to the observed hydrographs. Also the rainfall volume was much lower than what would be expected from the runoff volumes. Comparisons with neighboring rain gauges suggest that intensive rain bursts are sometimes missed by the rain gauge if the rainfall occurs locally. We therefore reconstructed a more plausible hyetograph from the neighboring rain gauge where a large rain burst did occur, although a little earlier which was then used for the simulations. There was a similar issue with the rainfall of the second largest event (8 August 1991) in the Wattenbach (Figure 10b) which we did not correct as the rain burst was less clear in the neighboring rain gauges.

#### 2.4.6. Step 4: Consistency Check of Calibrated Parameters With Field Information and Possibly Another Iteration of Step 1

[21] As a last step of parameter selection the calibrated parameters were rechecked for consistency with the field information (surface runoff response units and the hydrogeologic response units). The final parameters for the Weerbach catchment are listed in Table 1. The parameters of the Wattenbach catchment are in the same ranges. The simulations in Figures 8–10 have been performed with the final parameter set.

### 2.5. Stochastic Precipitation Model

[22] For the Monte Carlo simulations precipitation time series were generated by a slightly modified version of the stochastic rainfall model of *Sivapalan et al.* [2005]. The model generates discrete independent rainfall events whose arrival times, durations, average rainfall intensity and the within-storm intensity patterns are all random, governed by specified distributions with parameters assumed to be seasonally dependent. The model was calibrated using the precipitation series from the Wattener Lizum rainfall station located in the Wattenbach catchment (23 years and 5 min resolution). The calibration procedure was as follows [see *Viglione et al.*, 2012]: (1) the rainfall data were analyzed and the storm events were separated, (2) characteristics of the events (e.g., duration, average intensity, mass curve) were compiled and their statistics (i.e., mean, variance and their seasonal variability) were estimated, and (3) the parameters of the stochastic rainfall model were fitted to these statistics. Since there were a large number of events the model parameters were deemed to be robust. Details on the model, its calibration, and validation are given by *Viglione et al.* [2012].

### 3. Derived Distributions Through Monte Carlo Simulations

[23] The rainfall model and the runoff model were used in Monte Carlo simulations to generate runoff time series of 100,000 years at a resolution of 15 min. The 23 years of observed air temperatures were used all over again in order to simulate snow and evapotranspiration. As the largest floods in the two catchments are produced by rainfall alone without snow melt contributions this was assumed to be a justifiable simplification. The Monte Carlo simulations are consistent with the runoff data (Figure 11). This is no surprise since the parameters of the runoff model have been selected with much care. For both catchments the simulated flood frequency curve changes slope at around 30 years with significantly larger slopes at larger return periods. The

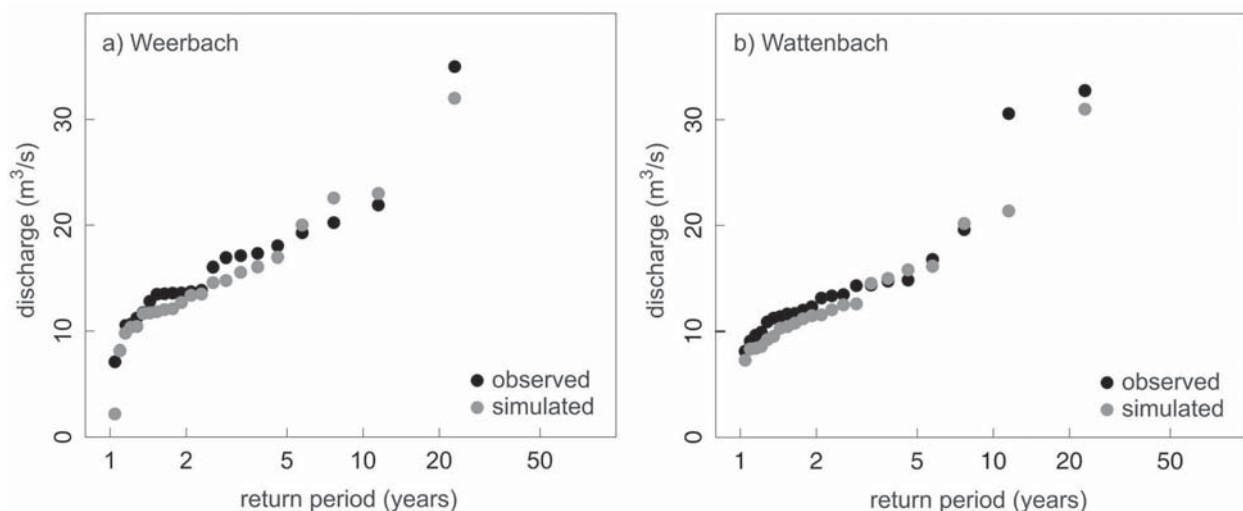


**Figure 10.** Flood frequency statistics of the observed versus simulated annual flood peaks in (a) the Weerbach and (b) Wattenbach catchments.

**Table 1.** Parameters for the Surface Runoff Response Units (SRRU) and the Hydrogeologic Response Units (HGRU) for the Weerbach Catchment

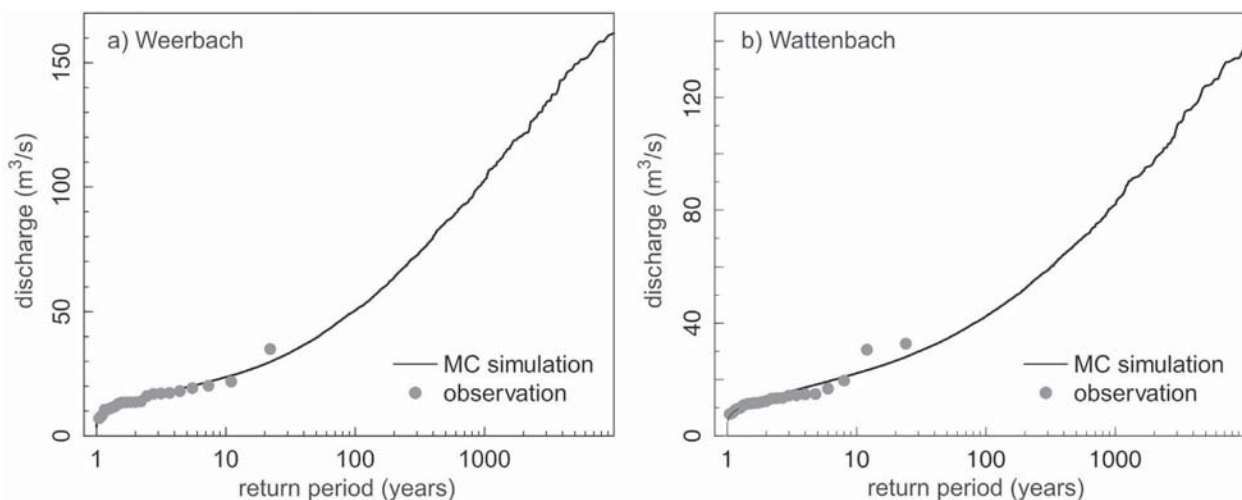
|  | SRRU       |         |            |           |           | HGRU                          |            |           |           |      |
|--|------------|---------|------------|-----------|-----------|-------------------------------|------------|-----------|-----------|------|
|  | $L_s$ (mm) | $\beta$ | $L_1$ (mm) | $k_0$ (h) | $k_1$ (h) | $c_p$ (mm d <sup>-1</sup> )   | $\alpha_p$ | $k_2$ (h) | $k_3$ (h) |      |
| Slow runoff, forest                      | 120        | 4       | 120        | 15        | 180       | Runoff in deep groundwater    | 16         | 0.6       | 600       | 1000 |
| Medium runoff, meadow                    | 100        | 4       | 110        | 10        | 150       | Runoff in shallow groundwater | 14         | 0.4       | 400       | 800  |
| Medium to fast runoff, alpine vegetation | 90         | 3       | 80         | 8         | 120       | Interflow                     | 10         | 0         | 300       | –    |
| Fast runoff, fast alpine vegetation      | 80         | 2       | 60         | 5         | 80        | Surface runoff on rocks       | 3          | 0         | 200       | –    |
| Very fast runoff, sealed area            | 10         | 1       | 5          | 3         | 30        | Runoff on saturated areas     | –          | –         | –         | –    |
| very fast runoff, Saturated area         | 10         | 1       | 10         | 5         | 30        |                               |            |           |           |      |
| No or very low runoff, talus material    | 5          | 1       | 200        | 50        | 200       |                               |            |           |           |      |
| Very fast runoff, rock                   | 30         | 1       | 10         | 5         | 30        |                               |            |           |           |      |

Monte Carlo simulations allow to analyze the process reasons for the change in slope of the distribution function in a more insightful way. Figure 12 shows areas contributing to fast surface runoff for events of different magnitudes in the Weerbach catchment. Surface runoff is defined as  $Q_0$  in the model. During smaller events (events 1 and 2) only very few areas contribute to direct surface runoff such as very fast runoff pixels, sealed areas and rocks. Between the second and third events, however, a strong increase in the contributing area from 8.7% to 47.9% can be observed. This sudden increase in the runoff contributing area can be related to the fact that the storage capacity of those areas is exceeded resulting in an increase in the slope of the distribution function. During even bigger events (events 4 and 5) the contributing area increases until almost the whole catchment contributes to direct surface runoff (event 5).

[24] Since the storage capacity of the catchment seems to have a crucial impact on the change in slope of the flood frequency curve, the storage behavior of the Weerbach catchment was analyzed by running additional simulations. Five further simulations were performed with five rainfall intensities that are constant in time ranging from 4 mm h<sup>-1</sup> to 20 mm h<sup>-1</sup>. At the beginning of each simulation, the storages were assumed to be empty. Figure 13 shows the simulated area contributing to fast surface runoff ( $Q_0$ ) plotted versus the event rainfall depth. As would be expected the contributing area increases with rainfall depth. For low

rainfall depths the rainfall intensity does not matter because the main mechanism is the filling of the subsurface storage. For larger rainfall depths higher intensities lead to earlier surface runoff. The increase of the area contributing to fast surface runoff with rainfall depth is not smooth, however. At a rainfall depth of about 150 mm a sudden increase in the surface runoff contributing area takes place. Below this value only a small amount of the catchment area generates surface runoff as shown also in Figure 12 events 1 and 2. As soon as the threshold is exceeded, a small increase in rainfall causes a large increase in the contributing area and hence in the surface runoff (see also Figure 12, event 3).

[25] The step change is hence caused by a threshold process, which is influenced by two factors. As shown in Figures 12 and 13, there is a sudden increase in the contributing area as soon as the storage capacity of these areas is exceeded. This means that the event volume is suddenly increased. This behavior can be interpreted as a sudden increase in the mean runoff coefficient of the catchment. Additionally, the runoff component  $Q_0$  that is activated by this process is significantly faster than the other runoff components ( $Q_1, Q_2, Q_3$ ). This means that the event is flashier than for smaller rainfall depths. This behavior can be interpreted as a sudden increase in the flow velocities of the catchment and therefore a decrease in the response time. For a step change such as the one in Figure 13 to occur, one would expect that the spatial distribution of the storage

**Figure 11.** Results of the Monte Carlo (MC) simulations for (a) the Weerbach and (b) Wattenbach catchments.

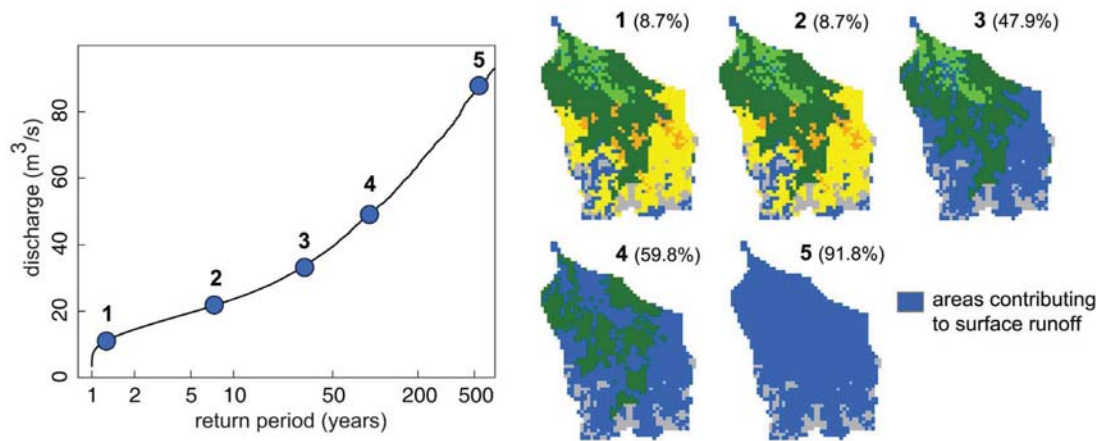


**Figure 12.** Runoff generation in the Weerbach catchment. (right) Areas contributing to fast surface runoff for events of different magnitudes. The percent contributing area is given in parentheses. (left) Simulated flood frequency curve with these events indicated.

capacity in part of the catchment is rather uniform. These areas will then “switch on” at the same time causing a step change in Figure 13 and therefore a similar change in the flood frequency curve. Note that in Figure 13 there is another change in slope around 300 mm which occurs when the catchment is fully saturated and no additional increase in the saturation area is possible.

**4. Discussion**

[26] The analysis of the two alpine catchments shows that step changes in the flood frequency curve are real and caused by the threshold behavior in the response of the hydrological system [Zehe and Sivapalan, 2009]. While a number of previous studies demonstrated this for hypothetical cases [Sivapalan et al., 1990; Blöschl and Sivapalan,

1997] the present paper demonstrates the presence of a step change for two real catchments.

[27] As Klemeš [1993] and Gutknecht [1994] suggest, runoff processes can be significantly different during small and big flood events. In this study the catchment area that contributes to a large flood event is significantly larger than the one contributing to a small flood event (Figure 12), which is equivalent with a low runoff coefficient for small events and a high runoff coefficient for large events. The contributing areas or runoff coefficients depend on the storage capacities of the catchments and were mainly described in the model by the use of hydrogeologic information. As the hydrogeologic runoff process maps show (Figure 6), both catchments have large areas with runoff in deep and shallow groundwater and consequently high storage capacities and only a few areas with a low storage capacity (i.e., the diversity of the storage capacity over the catchment is low). The storage behavior of the Weerbach catchment was analyzed in more detail applying synthetic rainfall events with constant rainfall intensities and the outcome shows that at a rainfall amount of approximately 150 mm, a sudden increase in the surface runoff contributing area takes place (Figure 13). This behavior can be interpreted as a threshold process when the spatial variability of storage capacity is low, i.e., the storage capacity in a large part of the catchment is rather uniform. The threshold triggers fast surface runoff from different runoff contributing areas. This is analogous to the threshold processes observed in experimental catchments when subsurface stormflow is activated [Detty and McGuire, 2010; Tromp-van Meerveld and McDonnell, 2006] and the switch from local infiltration to lateral flow in the study of Grayson et al. [1997]. Here subsurface storages are filled in a similar way, but fast surface runoff is activated on a number of areas at the same time. In addition to the distribution of the storage capacity, the magnitude of the storage capacity is important as it determines the return period at which the step change in the flood frequency curve occurs. If the storage capacity is much larger than extreme rainfall, the step change will only occur at extremely large return periods. If the storage capacity is much smaller, the step change will occur at

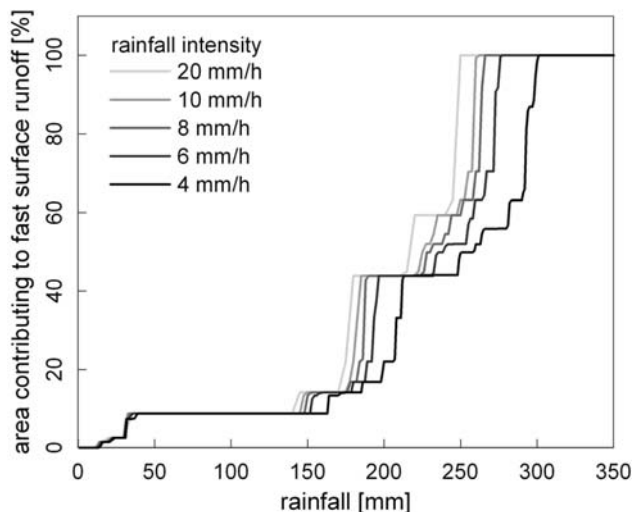


**Figure 13.** Simulated area contributing to fast surface runoff in the Weerbach for different event rainfall depths (horizontal axis). Rainfall intensities were assumed to be constant in time (five cases, 4–20 mm h<sup>-1</sup>).

small return periods and therefore not be of interest for the extrapolation of the flood frequency curve. For storage capacities similar to the most extreme rainfalls, as is the case in the study catchments, the step will occur at return periods of the largest events. This is the case which is of most interest for practical applications.

[28] While we did not analyze in detail the role of antecedent soil moisture [Zehe *et al.*, 2005] it is clear that the main control on the step change is the spatial distribution of the effective storage capacity, i.e., the volume that can be filled with water during an event for a given soil moisture state. If the antecedent soil moisture is high, less event rainfall is needed to reach saturation so one would expect some climate controls through soil moisture deficits or event runoff coefficients [Merz and Blöschl, 2009b]. Also, the spatial distribution of rainfall will play a role. Generally speaking step changes of the flood frequency curve are a manifestation of the nonlinearity of hydrological systems [Blöschl and Zehe, 2005].

[29] Another likely factor for the occurrence of a step change is the catchment scale. As the catchment size increases, the storage tends to become spatially more heterogeneous. Simultaneous saturation of a large part of the catchment is therefore less likely than in a small catchment. This is reflected in a slight decrease in the skewness of the observed flood peaks as a function of catchment area in Austria [Merz and Blöschl, 2009a]. On the basis of a derived flood frequency model, Blöschl and Sivapalan [1997] showed that a step change may move toward larger return periods with increasing catchment size because of decreasing catchment rainfall intensities. One would therefore expect threshold processes to have rather an effect in small catchments than in larger catchments where more averaging of the spatial hydrological variability occurs [Sivapalan, 2003]. A related question of scale is whether the chosen number of hydrological response units (Table 1) is necessary to explain the step change and whether a pixel size of 200 m is needed. In order to reproduce the main characteristics probably only two or three response units would be needed with much larger pixels or computational units. The limits of reducing complexity is when the shape of the storage function (Figure 13) can no longer be represented well. There are a number of studies suggesting that simpler model structures may suffice when one is only interested in the runoff at the catchment outlet but the main spatial characteristics within the catchment need to be represented by the model [e.g., Brath and Montanari, 2000; Blöschl *et al.*, 1995]. In the case of the step changes of the flood frequency curve in the catchments of this study the main spatial characteristic is the distribution of the storage capacity.

[30] It is clear that understanding the storage capacity and its spatial distribution is essential for ascertaining whether a step change in the flood frequency curve may occur or not. The present study has shown a road map of how the storages can be estimated from hydrogeologic field information. Without such detailed information it is more difficult to ascertain whether such a step change may occur. This is an important point for practical applications. We suggest that information on storage can be inferred from comparative analyses with catchments where either more detailed hydrogeological information or longer flood records are available. The idea of comparative hydrology is to compare catchments with contrasting characteristics in order to understand the controls in a holistic way rather than modeling a single catchment in much detail [Gaal *et al.*, 2012]. We compared the two catchments of this study with eight additional catchments in Tirol ranging in size from 4 km<sup>2</sup> to 98 km<sup>2</sup>. While in all of them hydrogeological assessments similar to the Wattenbach and the Weerbach were available, the catchments had contrasting hydrogeological characteristics. One of them had similar storage characteristics as the Weerbach with a similar step in the flood frequency curve. One of them had much larger storages without a step change and six others had less storage so, again, no step change occurred in the flood frequency curve. This means that out of a total of 10 catchments only three had the behavior analyzed in this paper and the others exhibited smooth flood frequency curves.

## 5. Implications for Design Flood Estimation

[31] The findings of this paper have important implications for design flood estimation. Assume that for a practical design task in the Weerbach catchment the 100 year design flood has to be estimated and that the presence of a step change is not known because no process-based analysis has been performed.

[32] The straightforward approach is to estimate the 100 year flood by fitting a distribution function to the flood peak data. Choice of the distribution function is usually subjective and checked by a goodness-of-fit test. Table 2 lists results of three model selection criteria [Laio *et al.*, 2009] for a number of commonly used distribution functions calculated for the Weerbach record. On the basis of these criteria one would choose the two-parameter Gumbel and lognormal distributions as these give the smallest numbers. Additionally the generalized extreme value (GEV) distribution can be considered which is the best among the three-parameter functions in Table 2. In this example we estimate the parameters of the three distribution functions

**Table 2.** Model Selection Criteria as by Laio *et al.* [2009]<sup>a</sup>

| Distribution Function | Number of Parameters | Akaike Information Criterion | Bayesian Information Criterion | Anderson-Darling Criterion |
|-----------------------|----------------------|------------------------------|--------------------------------|----------------------------|
| Normal                | 2                    | 142.6                        | 144.8                          | 0.58                       |
| Lognormal             | 2                    | 135.5                        | 137.7                          | 0.12                       |
| Gumbel                | 2                    | 135.3                        | 137.5                          | 0.11                       |
| Fréchet               | 2                    | 137.9                        | 140.1                          | 0.34                       |
| GEV                   | 3                    | 137.2                        | 140.5                          | 0.16                       |
| Pearson type III      | 3                    | 137.8                        | 141.1                          | 0.19                       |
| Log-Pearson type III  | 3                    | 137.3                        | 140.6                          | 0.17                       |

<sup>a</sup>Lower values correspond to more suitable models. GEV, generalized extreme value.

**Table 3.** The 100 Year Flood Estimates of the Gumbel, Lognormal, and GEV Distribution With 5% and 95% Confidence Bounds<sup>a</sup>

| Distribution Function | 100 Year Flood ( $\text{m}^3 \text{s}^{-1}$ ) | 5% Confidence Bound ( $\text{m}^3 \text{s}^{-1}$ ) | 95% Confidence Bound ( $\text{m}^3 \text{s}^{-1}$ ) |
|-----------------------|---|--|---|
| Gumbel                | 32  | 27   | 40  |
| Lognormal             | 33  | 27   | 45  |
| GEV                   | 34  | 28   | 53  |

<sup>a</sup>The shape parameter of the GEV distribution has been determined restricted to the statistically and physically reasonable range suggested by *Martins and Stedinger* [2000].

by the Bayesian method (using an MCMC algorithm [see, e.g., *Gaume et al.*, 2010]) which gives the 100 year flood peak with their 5%–95% confidence bounds (Table 3). For comparison, the 100 year flood estimate from the process-based derived flood frequency approach with a step change is  $50 \text{ m}^3 \text{ s}^{-1}$ . This value is much higher than the estimates of the three probability distributions (Table 3). Moreover, it is inconsistent with the Gumbel and Lognormal distributions since it lies outside the 95% confidence bound (Table 3). For the GEV distribution it is not inconsistent, but lies very close to the 95% confidence bound. This means that the estimate from the process-based derived flood frequency approach with a step change can differ significantly from the estimates of commonly used distribution functions if a step change in the data record is not apparent.

[33] Since the flood record of the Weerbach catchment is short one would probably recommend to use other information as well [e.g., *Merz and Blöschl*, 2008a, 2008b], for example by performing also a regional frequency analysis. The underlying assumption is that additional information on the probability of floods in the catchment of interest can be gained by observations in neighboring and/or similar catchments. If additional information is available, one could consider even more complex distribution functions such as mixed distributions (e.g., the TCEV distribution [Rossi et al., 1984]). Indeed, the parameters of mixed distributions are generally estimated from regional information such as extreme flood peaks in other flood records or extreme rainfall events in order to estimate the point of inflection well [e.g., *Rossi et al.*, 1984; *Hirschboeck*, 1987; *Gabriele and Arnell*, 1991; *Murphy*, 2001; *Guse et al.*, 2010]. If a step change is due to climatic or meteorological reasons (e.g., floods produced by usual storms versus floods produced by hurricanes), then analyzing data from more catchments in a region would be useful for identifying different flood types and fitting the parameters of a mixed distribution that reflects these controls. In the presented example the step change is due to the local geological setting. Pooling data from other catchments in the region would not be helpful, as the storage capacities in the catchments of the region differ (see section 4) so any step changes would be likely to average out. Instead the potential presence of a step change and its causes need to be ascertained through field analysis and the process-based methods presented in the paper.

## 6. Conclusions

[34] The study demonstrates that, in small catchments, step changes in the flood frequency curve can be real and

explained by the exceedance of storage thresholds at a critical rainfall depth. Because of this threshold the catchment area that contributes to a large flood event is significantly larger than the one contributing to a small flood event which is equivalent to a change of runoff coefficients from small to big events. A step change may occur when the storage capacity in a large part of the catchment is rather uniform and is of most interest when the storage capacity of a catchment is similar to the most extreme rainfall as it will occur around the return periods of the largest events. These are the events that need to be estimated for many hydrological applications. To assess the spatial distribution of storage capacities, hydro-geologic information is essential. This paper presents a road map of how the storage capacities can be estimated from field surveys.

[35] The potential presence of step changes in the flood frequency curve has important implications for hydrological design. When an outlier is present in a flood sample there are traditionally two options of dealing with it (Figure 14). The first is to assume that the outlier is real and representative of the sample (line 1 in Figure 14), i.e., one would assume that the flood frequency curve indeed increases steeply at the tail as a consequence of the rainfall-runoff processes in the catchment. The second option is to assume that the outlier is a result of sampling uncertainty, i.e., it should not be plotted at the plotting position consistent with the record length but at much larger return period. One would then probably extrapolate the flood frequency curve without taking the outlier into account (line 2 in Figure 14). A third option (line 3 in Figure 14) may be that the flood frequency curve indeed exhibits a step change with a sharp increase in the slope when the storage capacity in part of the catchment is exhausted and a decrease in the slope when only few additional areas get saturated with increasing return

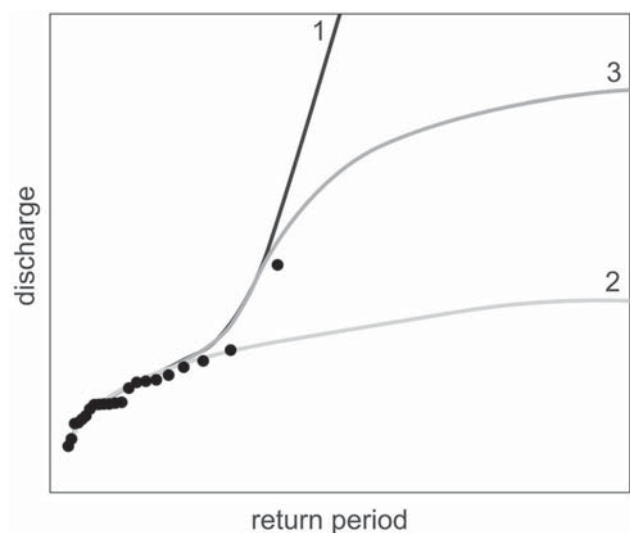


**Figure 14.** Different ways of extrapolating beyond a data sample: Extrapolation when (1) the outlier is considered to be real and representative of the sample, (2) it is considered a result of sampling uncertainty, and (3) it is considered real but the flood frequency curve exhibits a step change when the storage capacity is exhausted.

period. In these cases, fitting a smooth distribution function may lead to a significantly different flood estimate compared to process-based approaches that are able to identify the step change.

[36] On the basis of hydrogeologic information a process-based approach may be able to identify a complex shape of the flood frequency curve and facilitate the estimation of low-probability floods. The concept of flood frequency hydrology can help to ascertain the shape of the flood frequency curve [Merz and Blöschl, 2008a, 2008b]. These concepts are currently being implemented in the new flood estimation guidelines in Germany [Deutsche Vereinigung für Wasserwirtschaft, Abwasser und Abfall, 2012].

[37] **Acknowledgments.** We would like to acknowledge financial support from the Hydrographic Service Tyrol, the Austrian Forest Engineering Service in Torrent and Avalanche Control, Section Tyrol, and the AdaptAlp project (Flash Floods Tyrol project, HOWATI) as well as the Austrian Science Funds FWF (Doctoral Programme on Water Resource Systems, DK-plus W1219-N22).

## References

- Allamano, P., P. Claps, and F. Laio (2009), An analytical model of the effects of catchment elevation on the flood frequency distribution, *Water Resour. Res.*, *45*, W01402, doi:10.1029/2007WR006658.
- Bergström, S., and A. Forsman (1973), Development of a conceptual deterministic rainfall-runoff model, *Nord. Hydrol.*, *4*(3), 147–170.
- Blöschl, G., and M. Sivapalan (1997), Process controls on regional flood frequency: Coefficient of variation and basin scale, *Water Resour. Res.*, *33*(12), 2967–2980, doi:10.1029/97WR00568.
- Blöschl, G., and E. Zehe (2005), On hydrological predictability, *Hydrol. Processes*, *19*(19), 3923–3929.
- Blöschl, G., R. B. Grayson, and M. Sivapalan (1995), On the representative elementary area (REA) concept and its utility for distributed rainfall-runoff modeling, *Hydrol. Processes*, *9*, 313–330.
- Blöschl, G., C. Reszler, and J. Komma (2008), A spatially distributed flash flood forecasting model, *Environ. Model. Software*, *23*, 464–478, doi:10.1016/j.envsoft.2007.06.010.
- Brath, A., and A. Montanari (2000), The effects of the spatial variability of soil infiltration capacity in distributed flood modeling, *Hydrol. Processes*, *14*(15), 2779–2794.
- Detty, J. M., and K. J. McGuire (2010), Threshold changes in storm runoff generation at a till-mantled headwater catchment, *Water Resour. Res.*, *46*, W07525, doi:10.1029/2009WR008102.
- Deutsche Vereinigung für Wasserwirtschaft, Abwasser und Abfall (2012), Ermittlung von Hochwasserwahrscheinlichkeiten, *DWA Merkblatt M251*, Hennef, Germany, in press.
- Deutscher Verband für Wasserwirtschaft und Kulturbau (1996), Ermittlung der Verdunstung von Land- und Wasserflächen, *DVWK Merkblätter* 238, p. 35, Bonn, Germany.
- Dunne, T., and R. D. Black (1970), An experimental investigation of runoff production in permeable soils, *Water Resour. Res.*, *6*(2), 478–490, doi:10.1029/WR006i002p00478.
- Eagleson, P. S. (1972), Dynamics of flood frequency, *Water Resour. Res.*, *8*(4), 878–898, doi:10.1029/WR008i004p00878.
- Gaál, L., J. Szolgay, S. Kohnová, J. Parajka, R. Merz, A. Viglione, and G. Blöschl (2012), Flood timescales: Understanding the interplay of climate and catchment processes through comparative hydrology, *Water Resour. Res.*, *48*, W04511, doi:10.1029/2011WR011509.
- Gabriele, S., and N. Arnell (1991), A hierarchical approach to regional flood frequency analysis, *Water Resour. Res.*, *27*(6), 1281–1289, doi:10.1029/91WR00238.
- Gaume, E., L. Gaál, A. Viglione, J. Szolgay, S. Kohnová, and G. Blöschl (2010), Bayesian MCMC approach to regional flood frequency analyses involving extraordinary flood events at ungauged sites, *J. Hydrol.*, *394*(1–2), 101–117.
- Grayson, R. B., A. W. Western, F. H. S. Chiew, and G. Blöschl (1997), Preferred states in spatial soil moisture patterns: Local and non-local controls, *Water Resour. Res.*, *33*(12), 2897–2908, doi:10.1029/97WR02174.
- Guse, B., T. Hofherr, and B. Merz (2010), Introducing empirical and probabilistic regional envelope curves into a mixed bounded distribution function, *Hydrol. Earth Syst. Sci.*, *14*, 2465–2478, doi:10.5194/hess-14-2465-2010.
- Gutknecht, D. (1994), Extremhochwässer in kleinen Einzugsgebieten, *Oesterr. Wasser Abfallwirtsch.*, *46*, 50–57.
- Hirschboeck, K. K. (1987), Hydroclimatically-defined mixed distributions in partial duration flood series regional flood frequency analysis, in *Proceedings of the International Symposium on Flood Frequency and Risk Analyses 14–17 May 1986, Louisiana State University, Baton Rouge, U.S.A.*, pp. 199–212, D. Reidel, Dordrecht, Netherlands.
- Horton, R. E. (1933), The role of infiltration in the hydrological cycle, *Eos Trans. AGU*, *14*, 446–460.
- Katz, R. W., M. B. Parlange, and P. Naveau (2002), Statistics of extremes in hydrology, *Adv. Water Resour.*, *25*(8–12), 1287–1304, doi:10.1016/S0309-1708(02)00056-8.
- Klemes, V. (1993), Probability of extreme hydrometeorological events—A different approach, in *Proceedings of the Yokohama Symposium, Extreme Hydrological Events: Precipitation, Floods and Droughts, Yokohama, Japan, IAHS Publ.*, *213*, 167–176 pp., IAHS Press, Centre for Ecology and Hydrology, Wallingford, UK.
- Laio, F., G. Di Baldassarre, and A. Montanari (2009), Model selection techniques for the frequency analysis of hydrological extremes, *Water Resour. Res.*, *45*, W07416, doi:10.1029/2007WR006666.
- Markart, G., B. Kohl, B. Sotier, T. Schauer, G. Bunza, and R. Stern (2004), Provisorische Geländeanleitung zur Abschätzung des Oberflächenabflussbeiwertes auf alpinen Boden-/Vegetationseinheiten bei konvektiven Starkregen (Version 1.0), *BFW Dok.* 3, 83 pp., Bundesminister für Land- und Forstwirtschaft, Umwelt und Wasserwirtschaft, Vienna.
- Martins, E. S., and J. R. Stedinger (2000), Generalized maximum-likelihood based generalized extreme-value quantile estimators for hydrologic data, *Water Resour. Res.*, *36*(3), 737–744, doi:10.1029/1999WR900330.
- McGuire, K. J., J. J. McDonnell, M. Weiler, C. Kendall, B. L. McGlynn, J. M. Welker, and J. Seibert (2005), The role of topography on catchment-scale water residence time, *Water Resour. Res.*, *41*, W05002, doi:10.1029/2004WR003657.
- Merz, R., and G. Blöschl (2003), A process typology of regional floods, *Water Resour. Res.*, *39*(12), 1340, doi:10.1029/2002WR001952.
- Merz, R., and G. Blöschl (2008a), Flood frequency hydrology: 1. Temporal, spatial, and causal expansion of information, *Water Resour. Res.*, *44*, W08432, doi:10.1029/2007WR006744.
- Merz, R., and G. Blöschl (2008b), Flood frequency hydrology: 2. Combining data evidence, *Water Resour. Res.*, *44*, W08433, doi:10.1029/2007WR006745.
- Merz, R., and G. Blöschl (2009a), Process controls on the statistical flood moments - a data based analysis, *Hydrol. Processes*, *23*(5), 675–696.
- Merz, R., and G. Blöschl (2009b), A regional analysis of event runoff coefficients with respect to climate and catchment characteristics in Austria, *Water Resour. Res.*, *45*, W01405, doi:10.1029/2008WR007163.
- Murphy, P. J. (2001), Evaluation of mixed-population flood-frequency analysis, *Hydrol. Eng.*, *6*(1), 62–70.
- Nielsen, S. A., and E. Hansen (1973), Numerical simulation of the rainfall-runoff process on a daily basis, *Nord. Hydrol.*, *4*(3), 171–190.
- Reszler, C., J. Komma, G. Blöschl, and D. Gutknecht (2006), Ein Ansatz zur Identifikation flächendetailierter Abflussmodelle für die Hochwasservorhersage, *Hydrol. Wasserbewirtsch.*, *50*(5), 220–232.
- Rossi, F., M. Fiorentino, and P. Versace (1984), Two-component extreme value distribution for flood frequency analysis, *Water Resour. Res.*, *20*(7), 847–856, doi:10.1029/WR020i007p00847.
- Sivapalan, M. (2003), Process complexity at hillslope scale, process simplicity at the watershed scale: Is there a connection?, *Hydrol. Processes*, *17*(5), 1037–1041.
- Sivapalan, M., E. F. Wood, and K. Beven (1990), On hydrologic similarity: 3. A dimensionless flood frequency model using a generalized geomorphologic unit hydrograph and partial area runoff generation, *Water Resour. Res.*, *26*(1), 43–58, doi:10.1029/89WR01579.
- Sivapalan, M., G. Blöschl, R. Merz, and D. Gutknecht (2005), Linking flood frequency to long-term water balance incorporating effects of seasonality, *Water Resour. Res.*, *41*, W06012, doi:10.1029/2004WR003439.
- Tromp-van Meerveld, H. J., and J. J. McDonnell (2006), Threshold relations in subsurface stormflow: 2. The fill and spill hypothesis, *Water Resour. Res.*, *42*, W02411, doi:10.1029/2004WR003800.
- Viglione, A., R. Merz, and G. Blöschl (2009), On the role of the runoff coefficient in the mapping of rainfall to flood return periods, *Hydrol. Earth Syst. Sci.*, *13*(5), 577–593.

- Viglione, A., A. Castellarin, M. Rogger, R. Merz, and G. Blöschl (2012), Extreme rainstorms: Comparing regional envelope curves to stochastically generated events, *Water Resour. Res.*, *48*, W01509, doi:10.1029/2011WR010515.
- Whipkey, R. Z. (1965), Subsurface stormflow from forested slopes, *Bull. Int. Assoc. Sci. Hydrol.*, *10*, 74–85.
- Zehe, E., and G. Blöschl (2004), Predictability of hydrologic response at the plot and catchment scale: Role of initial conditions, *Water Resour. Res.*, *40*, W10202, doi:10.1029/2003WR002869.
- Zehe, E., and M. Sivapalan (2009), Threshold behaviour in hydrological systems as (human) geo-ecosystems: Manifestations, controls, implications, *Hydrol. Earth Syst. Sci.*, *13*(7), 1273–1297.
- Zehe, E., R. Becker, A. Bárdossy, and E. Plate (2005), Uncertainty of simulated catchment runoff response in the presence of threshold processes: Role of initial soil moisture and precipitation, *J. Hydrol.*, *315*(1-4), 183–202, doi:10.1016/j.jhydrol.2005.03.038.
- 
- G. Blöschl, R. Kirnbauer, J. Komma, M. Rogger, and A. Viglione, Institute for Hydraulic Engineering and Water Resources Management, Vienna University of Technology, Karlsplatz 13, A-1040 Vienna, Austria. (rogger@hydro.tuwien.ac.at)
- B. Kohl, Department of Natural Hazards and Alpine Timberline, Federal Research and Training Centre for Forests, Natural Hazards and Landscape, Hofburg, Rennweg 1, A-6020 Innsbruck, Austria.
- R. Merz, Department for Catchment Hydrology, Helmholtz Centre for Environmental Research, Theodor-Lieser-Straße 4, D-06120 Halle, Germany.
- H. Pirkl, Technical Office for Geology Dr. Herbert Pirkl, Plenergasse 5/27, A-1180 Vienna, Austria.